Space–time dynamics of local scour around submerged tandem and staggered piers in sand beds

L. N. Pasupuleti[1], P. V. Timbadiya[2,*] and P. L. Patel[2]

[1]Department of Civil Engineering, Aditya Engineering College, Surampalem 533 437, India
[2]Department of Civil Engineering, Sardar Vallabhbhai National Institute of Technology, Surat 395 007, India

Experimental studies on temporal variations around submerged piers on sand beds are compared here with the findings of an isolated pier under identical flows. Scour depths at the rear pier of the tandem case were found to decrease by 40% compared to the isolated pier. On the other hand, the scour depth around the staggered rear pier was similar to the isolated pier. From bed gradient computations, the mean of the highest gradients at deeper and upstream portions of the scour hole was approximately equal to the angle of repose in the isolated pier. The dynamic angle of repose increased by 20% and 40% in the front piers of the tandem and staggered arrangements respectively, vis-à-vis the isolated pier, leading to the rapid movement of sediments between the piers.

Keywords: Angle of repose, local scour, sand bed, space–time dynamics, staggered piers, tandem and staggered piers.

PRECISE estimation of maximum scour depth is required for the safety of bridge piers. Space–time dynamics of local scour around the parallel bridge piers, particularly those arranged in tandem and staggered configuration, is a challenging topic of study in hydraulic engineering. Local scour around the bridge piers has been reported in previous studies through extensive experimentation using point gauges in the laboratory flume[1–3] (see Figure 1 for mechanisms of local scour). Moreover, mathematical models were developed to predict maximum scour depth around the piers[4–9]. Recently, Sheppard *et al.*[10] conducted experiments on their developed model, assessing 454 datasets with intricate pier geometries. They employed a diverse set of complex pier shapes to estimate local scour. The effect of interference in tandem and staggered pier arrangements has been determined[11,12]. Ravanfar *et al.*[13] found that scour depth in non-uniform tandem piers was higher than in uniform piers; staggered piers showed more scour depth than tandem piers. Studies are scarce in the literature on quantifying local scour in the space–time domain around submerged tandem piers using recent and precise instruments such as URS (ultrasonic ranging system) on sediment beds (Figure 2). Moreover, studies on staggered piers using URS are completely missing in the literature. Instantaneous bed elevation was measured using the SeaTek 5 MHz URS composed of 32 transducers (Tr) around isolated, tandem and staggered piers. The present study analyses the interference of downstream piers in tandem and staggered arrangements on the evolution of scour holes around an upstream pier on a uniform sediment bed using concurrent bed-level measurements employing URS (see Figure 3 for pier arrangement). Also, intercomparison of the space–time dynamics of local scour around the aforesaid pier arrangements was made for identical flow conditions to better understand flow physics/hydraulics around the piers. Temporal variations of local scour at different time intervals and scour hole gradients around isolated, tandem and staggered piers are also presented in this study. The study provides insights into concurrent, instantaneous bed-level variations around isolated, tandem and staggered piers on

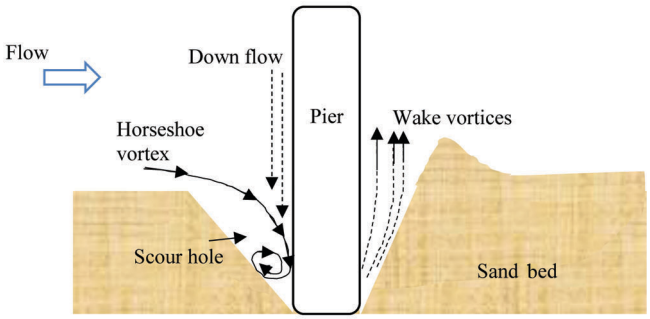

Figure 1. Schematic of flow fields around the isolated pier.

Figure 2 *a*, *b*. Photographs showing (***a***) transducers placed at different arrays on the trolley and (***b***) allied data acquisition system.

*For correspondence. (e-mail: pvtimbadiya@ced.svnit.ac.in)

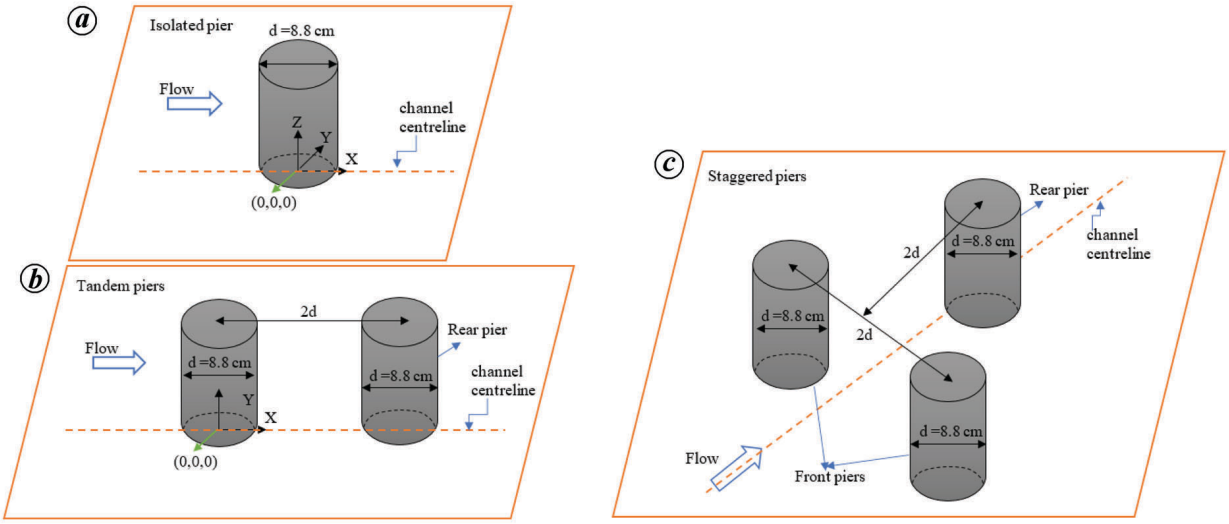

Figure 3. Sketch of (***a***) isolated pier, (***b***) tandem pier and (***c***) staggered pier arrangements.

sand beds. Understanding such bed-level variations would help in making a qualitative decision on selecting the alignment of piers in parallel bridges.

Experimentation

Experiments were conducted in a re-circulating sediment transport flume (15 m long, 0.89 m wide and 0.6 m deep) at the Advanced Hydraulics Laboratory, Sardar Vallabhbhai National Institute of Technology, Surat, Gujarat, India (Figure 4)[14]. A 6.0 m long working section, having side walls made up of perspex glass to view the flow, was located 5.0 m downstream from the inlet of the flume. A tailgate was used to adjust the required flow depth and maintain uniform flow in the working section. Discharge in the channel was adjusted using the SCADA (supervisory control and data acquisition) system, which has been designed to maintain a steady, uniform flow in the channel.

Materials and methods

The sediment bed of 15 cm thickness was laid in the working section of the flume. Uniform sediments with mean size, $d_{50} = 0.75$ mm, standard deviation $\sigma_g = 1.29$, specific gravity of 2.65, angle of repose $\phi = 31.5°$ and critical bed shear stress $\tau_{bc} = 0.424$ N/m^2 were used during the experiments. The upstream pier was located 8.0 m from the inlet of the flume to ensure the fully developed flow condition upstream of the pier. The rear pier in the tandem case was positioned at S/d ratio = 2 (centre-to-centre distance = 17.6 cm).

Here, S is the centre-to-centre distance between the piers in the longitudinal direction. Such spacing was decided based on previous studies, which highlighted that critical spacing with reference to the maximum scour depth is 2–3 times the diameter of the pier[4,11,12]. With such spacing, the rear pier interacts with the vortex shedding of the upstream pier, which amplifies the vortex under certain conditions[15]. Further, at spacing $S/d = 2$, both upstream and downstream piers will not behave as isolated piers. Ataie-Ashtiani and Ataie-Kordkandi[16] performed similar experimental studies on flow fields around tandem piers at $S/d = 3$.

In a staggered arrangement, two piers are located upstream of the third pier, which is located downstream between the two piers (Figure 3 *c*). The size of the pier was chosen such that the ratio of channel width to pier diameter was more than 6.25 to avoid contraction effects[6]. The same was followed for the isolated and tandem piers also. The ratio of flow depth to pier diameter is known as the shallowness factor. The limiting value of this factor is 3; beyond this, the scour around a pier is independent of flow depth[7]. During experimentation, the ratio (Z_0/d) in the present study was maintained at 1.2. Here, Z_0 is the approaching flow depth, which was 10.5 cm in the present study. Further, relative sediment coarseness (d/d_{50}) was maintained at 117 during the experiments. The limiting value for the aforesaid ratio is 50; below this limit, the scour around a pier becomes independent of sediment size[17]. The intensity of the flow (U/U_c) in the present study was maintained as 0.93, wherein the critical velocity (U_c) is 0.286 m/s, measured using the Schamovis equation[18]. U is the depth-averaged approaching flow velocity (0.268 m/s) determined from the measured velocity profile at 1 m upstream of the upstream pier, where the presence of the pier did not affect the flow. Clear-water condition was maintained in the approaching flow in the working section by setting the velocity lower than the sediment threshold (i.e. $U_*/U_{*c} \approx 0.97$), where $U_{*c} = 0.019$ m/s is the critical shear velocity[19] and U_* (0.0186 m/s) is the shear velocity measured from the

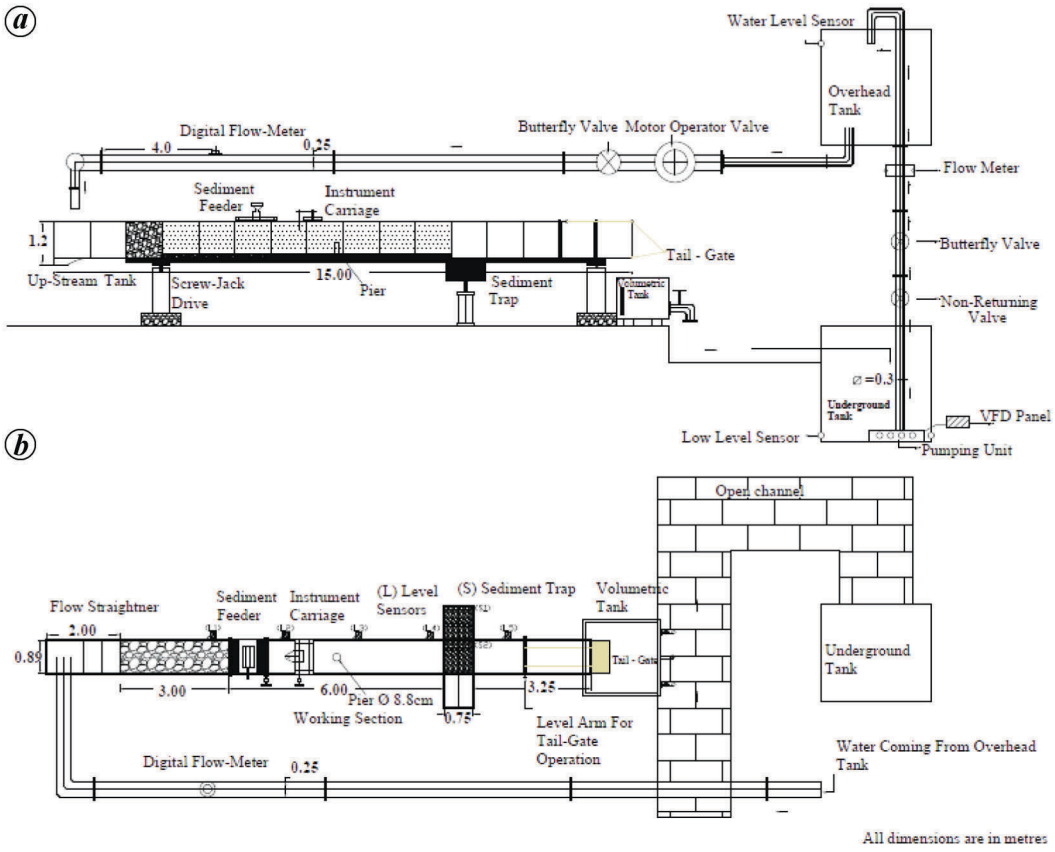

Figure 4. Schematic of experimental set-up: (***a***) elevation and (***b***) plan.

measured velocity profile[16]. Further, other flow conditions like Froude number (F_r = 0.264), densimetric Froude number (Fd_{50} = 2.432) and flow Reynolds number (Re = 2.4 × 10^4) were maintained during the experiments.

All 32 transducers were mounted on a plate and submerged in the water over the piers with the help of a trolley (Figure 5). The concurrent bed deformations were continuously recorded at a sampling frequency of 4.0 Hz. It was seen that the sand bed attained stable conditions in 360, 600 and 720 min for the isolated pier, front piers of tandem and staggered cases respectively. Beyond this time interval, the bed elevations were recorded, which were within ± 1.0 mm/h. Hence, the conditions of the bed were considered to be in a quasi-equilibrium state in the present study. A similar criterion for quasi-equilibrium state was considered by Dey *et al.*[7].

Results and discussion

Scour depth around upstream piers

The observed quasi-equilibrium scour depth around the isolated pier was compared with those reported by Sarkar *et al.*[20,21], with good agreement (Figure 6 *a*). Also, the quasi-equilibrium state for the front pier of the tandem arrangement was compared with that reported by Chavan *et al.*[22], with good agreement (Figure 6 *b*). The quasi-equilibrium state for the submerged front piers of the staggered arrangement has not been examined in previous studies. Further, in tandem piers, at S/d = 2, scour depths were observed to be 15% more around the front pier when compared to the isolated pier. The front pier, in the tandem case, experienced an increase in strength of the horseshoe vortex, leading to a larger scour depth compared to the isolated pier. Keshavarzi *et al.*[12] also reported similar observations at S/d = 2.5 for the tandem pier arrangements. It can be observed from Figure 6 *d* that the quasi-equilibrium scour depth (d_{se}) in the staggered front pier is 38% higher than that of the isolated pier for similar flow conditions.

Scour depth around rear piers

In the tandem arrangement, the maximum scour depth around the rear pier was compared with that reported by Chavan *et al.*[22], and we found good agreement for the corresponding time intervals. The scour depth in the rear pier in the tandem case was found to be 40% lower than that for the isolated pier for the corresponding flow conditions due to sheltering effect, i.e. the bed material from the scour hole of the front pier is deposited in the scour hole of the

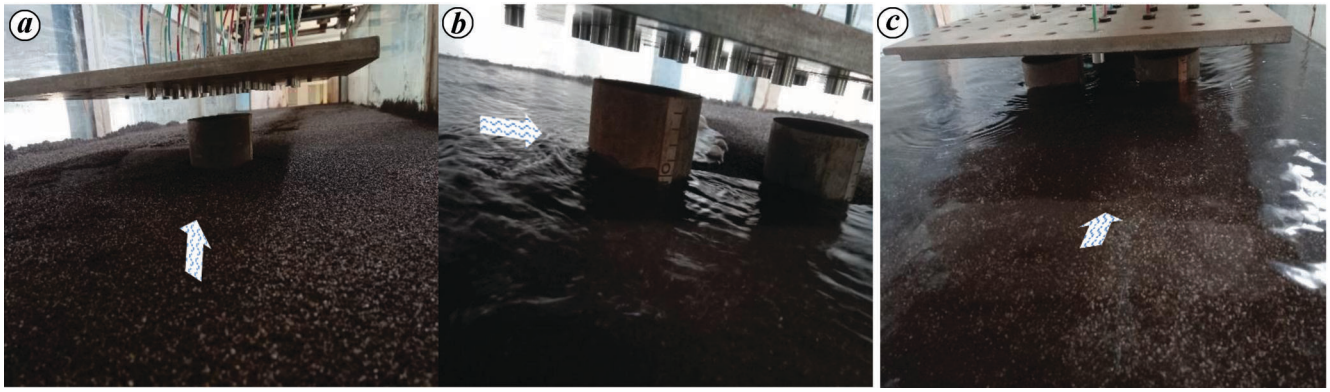

Figure 5 *a*–*c*. Photographs taken during data collection. The transducer positions over (***a***) the isolated pier, (***b***) tandem piers and (***c***) staggered piers.

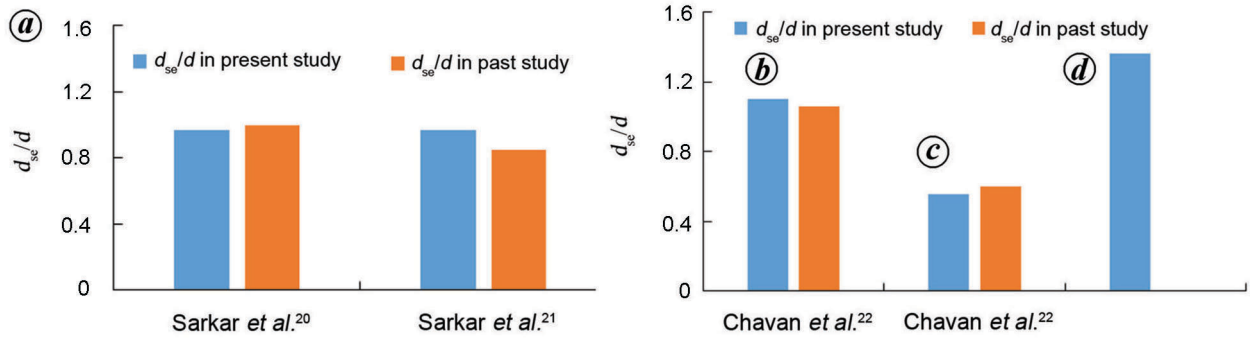

Figure 6. Comparison of quasi-equilibrium scour depth of the present study with previous studies for (***a***) isolated pier, (***b***) front pier of tandem case, (***c***) rear pier of tandem case and (***d***) staggered front pier.

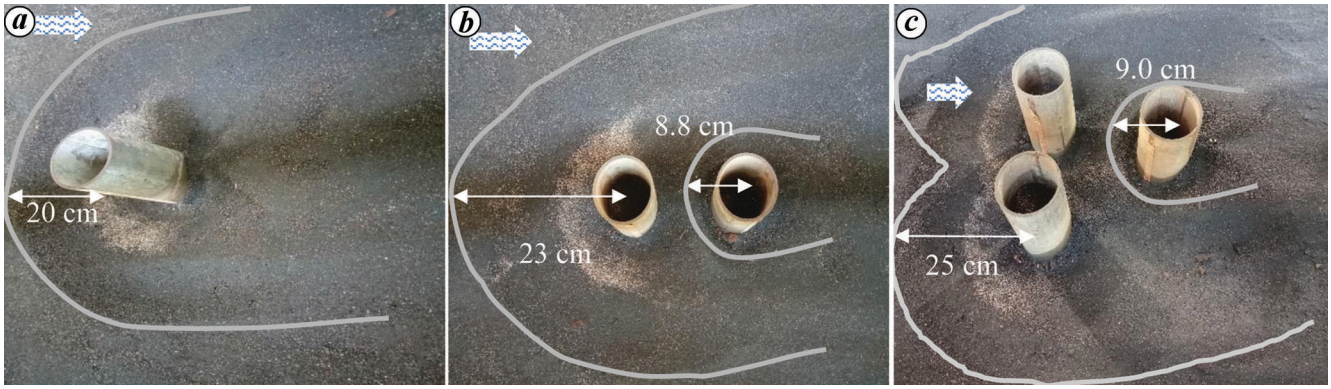

Figure 7 *a*–*c*. Photographs showing final deformed bed around. ***a***, isolated pier; ***b***, tandem piers; ***c***, staggered piers.

rear pier, which leads to a reduction in scour depth of the rear pier (Figure 6 *c*). On the other hand, the scour depths were similar for both the staggered rear pier and the isolated pier. Figure 7 shows photographs of the final deformed area around the isolated, tandem and staggered piers. It can be seen from Figure 7 that patterns of scour holes around the isolated pier and tandem front piers are almost similar. In the present study, the experimental observations around front pier in tandem case are similar to those of Chavan *et al.*[22]. On the other hand, the scour structure had significantly changed in case of the tandem rear pier. The radius of scour holes was 2.2 and 2.65 times more in isolated and tandem front piers respectively, compared to the tandem rear piers (Table 1).

Further, the ratio of radius of scour in longitudinal direction and transversal direction were slightly higher for the staggered rear pier than the tandem rear pier. The higher scour hole radius around staggered piers is due to

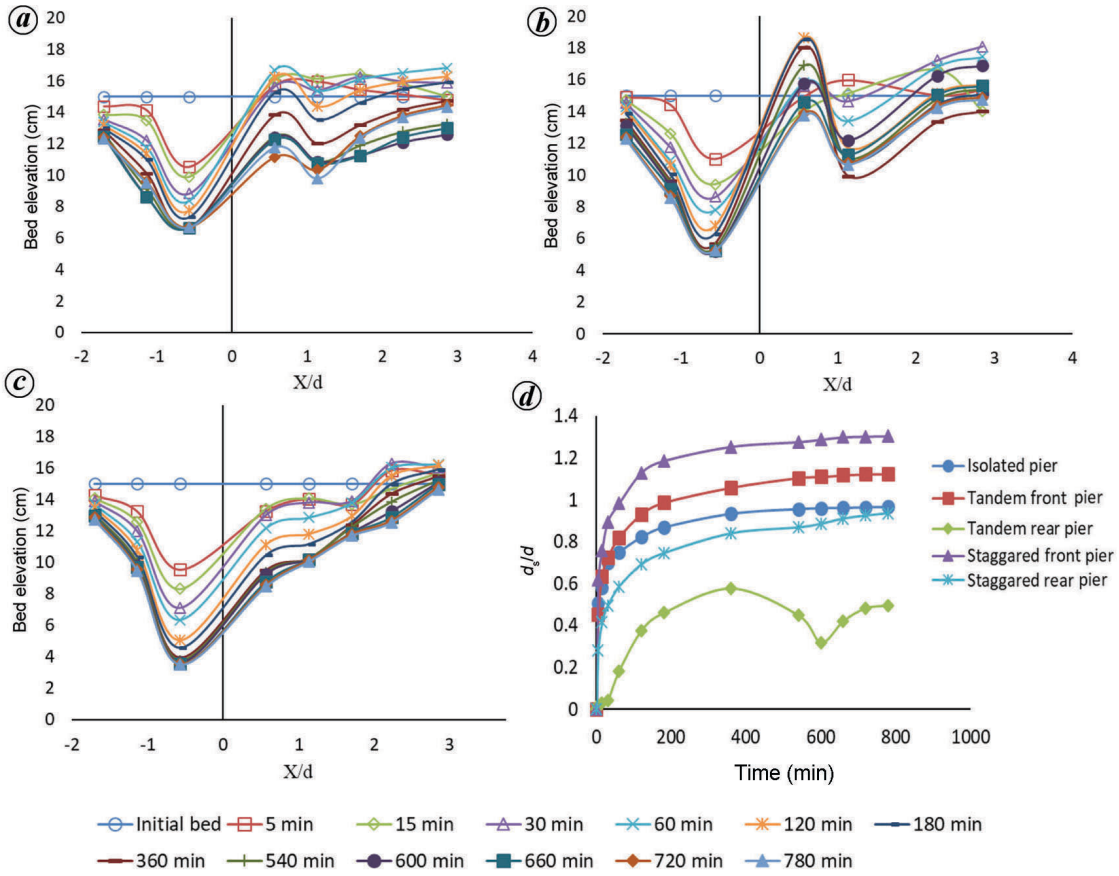

Figure 8. Temporal variations in bed elevation for (***a***) isolated pier, (***b***) tandem front pier and (***c***) staggered front piers. (***d***) Temporal variation of the ratio of scour depth to pier diameter around the piers in all three configurations.

Table 1. Scale measurement of final deformed beds around the piers

	Longitudinal direction	Transverse direction
Scour radius (distance from pier centre; cm)		
Isolated pier	20	20
Tandem front pier	23	23
Tandem rear pier	8.8	8.8
Staggered front pier	25	25
Staggered rear pier	9	9
Affected deformed zone (cm)		
Isolated pier	80	50
Tandem piers	167	55
Staggered piers	210	77

more exposure of the rear pier to the approaching flow compared to the rear pier of the tandem arrangement.

Temporal variations of bed elevation around the piers

Figure 8 presents the temporal variations of the bed along the centreline of the piers at different time intervals. For the isolated pier, the initial 15-min scour depth was observed to be 5.0 cm, which reveals the rapid deformation of the sediment bed. Thereafter, the deformation was gradual, and the bed retained a stable shape after 360 min. Beyond this time interval, the bed elevation changes were recorded within ± 2.0 mm. For the tandem front pier, rapid bed deformation was observed within an initial 5 min and scour depth up to 4.0 cm was observed within that time interval. Further, up to 180 min, the sediment bed deformed rapidly, and a scour depth of up to 8.7 cm was observed. Beyond this time interval, the bed had gradually deformed, and stable bed condition was reached at 600 min. The observations on staggered piers revealed that a scour depth of 5.5 cm was reached within the initial 5 min which was more rapid than in the tandem case. Further, a 10 cm scour depth was reached in 180 min. Beyond this time interval, the sediment bed was gradually deformed slowly and reached a stable condition at 720 min with a scour depth of 12 cm. The lowest bed elevation from the channel bottom was observed at the transducer location Tr-16 (located 0.2 cm from the periphery of the pier) in both isolated and tandem front pier. For the staggered front pier, the lowest bed elevation was observed at Tr-8 and Tr-29. On the other hand, the highest bed elevation was observed at Tr-3 and Tr-30 (1.0 cm downstream from the periphery of the pier). Similarly, for the isolated and tandem front piers, the highest

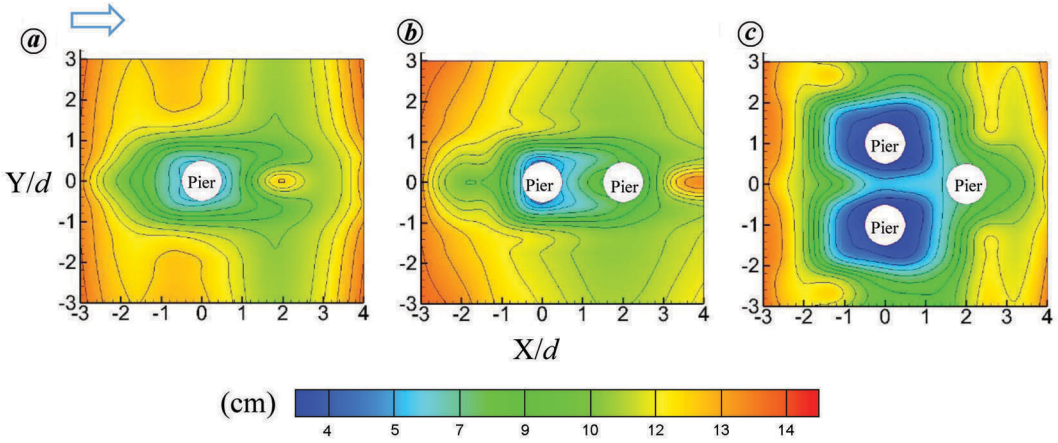

Figure 9. Surface contour plots of bed elevation at the end of run for (***a***) isolated pier, (***b***) tandem piers and (***c***) staggered piers.

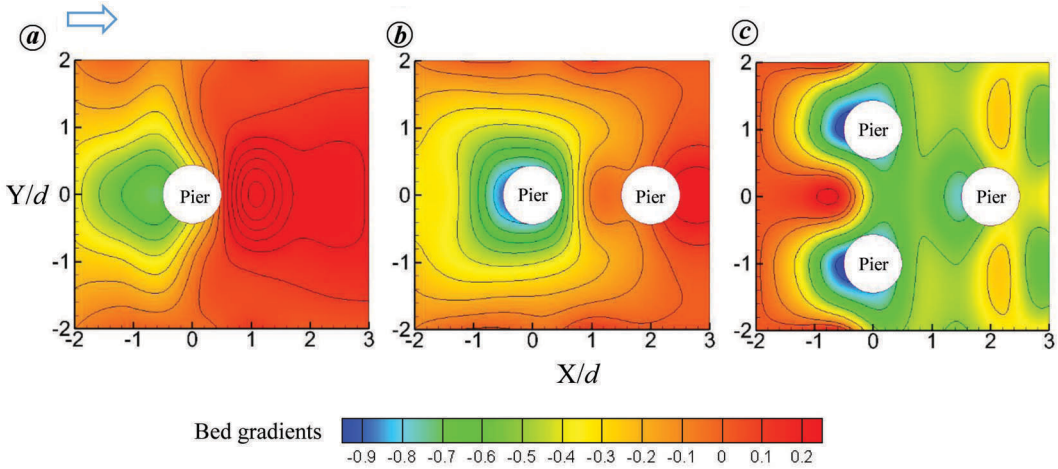

Figure 10. Contour plots of bed gradient along the flow at the end of run for (***a***) isolated pier, (***b***) tandem piers and (***c***) staggered piers.

bed elevation was observed at Tr-17. For the tandem rear pier, the bed deformation was rapid at all time intervals. It was observed that sediment particles were infilled in the scour hole due to scoured bed material from the front pier. A scour depth of 5.0 cm was observed for the tandem rear pier at 360 min in Tr-18 (2.8 cm from the pier periphery). Beyond this time interval, the scour depth gradually decreased, and it was 2.8 cm at 600 min. From Figure 8 *d*, it can be observed that there is a dip in the time variation plot of the scour around the rear pier. The scoured bed material from the front pier is initially deposited behind the same pier. After a certain time interval, this material reaches the scour hole of the rear pier, which causes a decrease in scour depth around the pier. Once again, scour depth increases and reaches 4.0 cm at 720 min. The rear pier of the staggered arrangement was found to gradually increase in scour depth and matched the quasi-equilibrium scour depth of the isolated pier. The decrease in scour depth around the rear pier at spacing ($S/d = 2$) was due to the combined action of the sheltering effect of the front pier and the deposition of sediments due to scoured material around the front piers.

Figure 8 *d* presents the non-dimensional scour depth, i.e. scour depths normalized with pier diameter at isolated, tandem and staggered piers, where d_s is the scour depth at time t.

Figure 9 shows the bed elevation contours at quasi-equilibrium conditions around the piers. Within the scoured region upstream of the isolated pier the streamwise velocity component was negative with a negative bed slope (stoss-faced) and gradually became positive downstream of the pier, where the sediment deposited with a positive bed slope (leeside face; Figure 9 *a*). Furthermore, the concentration of bed-level contour lines was greater upstream of the front pier for the staggered arrangement (Figure 9 *c*). This suggests that the magnitude of velocity in that region changes rapidly compared to the tandem and isolated pier arrangements. Hence, the combined effect of the highest

velocities on either side leads to more scour around the front piers.

Figure 10 shows the contours of bed gradients around the piers along the flow direction at the end of the run. From Figure 10 *a*, at the stoss-faced slope, the highest gradient (dynamic angle of repose) is found to be –0.69 (–34.6°) and –0.47 (25.17°) at the deeper and upper parts of the scour hole respectively. The gradients for the isolated pier in the present study are comparable with those of Sarkar *et al.*[20]. Further, the mean (29.89°) of the highest gradient at the upper and deeper portions of the scour hole is approximately equal to the angle of repose[23]. The dynamic angle of repose at a quasi-equilibrium state in the present study is found to be 16% higher than the angle of repose. According to Dey *et al.*[7], the dynamic angle of repose at the quasi-equilibrium state is 15–20% higher than the angle of repose. Therefore, the gradients in the isolated pier case are consistent with the findings reported in earlier studies[7,20].

For the tandem front pier, the gradients are increased by 20% vis-à-vis the isolated pier case (Figure 10 *b*). It can be seen from the figure that, at deeper parts of the scour hole, the highest gradient is –42°, while in the upper portion, the highest gradient is found to be –34°. On the other hand, the gradients are 1.2 times more at staggered in the front piers vis-à-vis the tandem front pier.

The scale measurements shown in Figure 7 *c* indicate the large size of the scour hole in the front piers of the staggered arrangement compared to the isolated pier and tandem pier arrangement. This is likely due to the larger size and strength of horseshoe vortices in the staggered front piers, which needs to be ascertained using flow-visualization techniques. However, due to the increase in the dynamic angle of repose in both front piers of tandem and staggered arrangements, the angle of repose is inconsistent with the gradients observed in the front piers for both cases.

Conclusion

An experimental study to quantify the space–time dynamics of local scour around submerged tandem and staggered piers in uniform mobile beds were carried out. The conclusions, along with the limitations of this study, are listed below:

(i) The quasi-equilibrium scour depths of the isolated pier and tandem front pier and the maximum scour depth of the rear pier in the tandem arrangement were compared with previous studies and found to be in good agreement.

(ii) The quasi-equilibrium scour depth (stable) was obtained in 360 min, and the corresponding scour depth was 8.7 cm for the isolated pier. On the other hand, for the front piers of tandem and staggered arrangements, the observed quasi-equilibrium scour depth was 10 cm at 600 min and 12 cm at 720 min. Moreover, 50% of the scour depth was reached in the initial 10 min for both cases.

(iii) The maximum scour depth around the tandem rear pier was found to decrease by 50% vis-à-vis the tandem front pier due to the combined influence of sheltering effect and deposition of sediments eroded from the front pier. On the other hand, sediment deposition was maximum between the front and rear piers of the tandem arrangement compared to that behind the isolated pier and staggered arrangement.

(iv) The mean of the highest gradients at the deeper portion (dynamic angle of repose) and upper portion of the scour hole was close to the angle of repose for the isolated pier. Also, in the front piers of the tandem and staggered arrangements, the dynamic angle of repose was 20% and 40% higher respectively, than that of the isolated pier due to the rapid movement of sediments between the piers in the tandem and staggered arrangements.

A single experimental run was performed for each pier configuration. Hence, the effect of scale on the space–time dynamics of the local scour and was not determined out in the present study, which can be considered in a future study.

1. Elliot, K. R. and Baker, C. J., Effect of pier spacing on scour around bridge piers. *J. Hydraul. Eng.*, 1985, **111**(7), 1105–1109.
2. Chiew, Y, M. and Melville, B. W., Local scour around bridge piers. *J. Hydraul. Res.*, 1987, **25**(1), 15–26.
3. Melville, B. W. and Chiew, Y. M., Time scale for local scour at bridge piers. *J. Hydraul. Eng*., 1999, **125**(1), 59–65.
4. Ataie-Ashtiani, B. and Beheshti, A. A., Experimental investigation of clear-water local scour at pile groups. *J. Hydraul. Eng.*, 2006, **132**(10), 1100–1104.
5. Moreno, M., Maia, R. and Couto, L., Prediction of equilibrium local scour depth at complex bridge piers. *J. Hydraul. Eng.*, 2016, **142**(11), 04016045.
6. Raudkivi, A. J. and Ettema, R., Clear-water scour at cylindrical piers. *J. Hydraul. Eng.*, 1983, **109**(3), 338–350.
7. Dey, S., Bose, S. K. and Sastry, G. L., Clear water scour at circular piers: a model. *J. Hydraul. Eng.*, 1995, **121**(12), 869–876.
8. Kothyari, U. C., Garde, R. C. J. and Ranga Raju, K. G., Temporal variation of scour around circular bridge piers. *J. Hydraul. Eng.*, 1992, **118**(8), 1091–1106.
9. Vijayasree, B. A. and Eldho, T. I., A modification to the Indian practice of scour depth prediction around bridge piers. *Curr. Sci.*, 2021, **120**(12), 1875–1888.
10. Sheppard, D. M., Melville, B. and Yang, Y., Local equilibrium sediment scour prediction at bridge piers with complex geometries. *J. Hydraul. Eng.*, 2023, **149**(4), 04023003.
11. Khaple, S., Hanmaiahgari, P. R., Gaudio, R. and Dey, S., Interference of an upstream pier on local scour at downstream piers. *Acta Geophys.*, 2017, **65**(1), 29–46.
12. Keshavarzi, A., Shrestha, C. K., Melville, B., Khabbaz, H., Ranjbar-Zahedani, M. and Ball, J., Estimation of maximum scour depths at upstream of front and rear piers for two in-line circular columns. *Environ. Fluid Mech*., 2018, **18**(2), 537–550.
13. Ravanfar, A. M., Mahammadpour, R. and Sabzevari, T., Experimental study of local scour around non-uniform twin piers. *J. River Basin Manage.*, 2023, 1–35.
14. Pasupuleti, L. N., Timbadiya, P. V. and Patel, P. L., Bed level variations around the submerged tandem piers in sand beds. *ISH J. Hydraul. Eng.*, 2020, **28**(1), 149–157.
15. Zhou, K., Duan, J. G. and Bombardelli, F. A., Experimental and theoretical study of local scour around three-pier group. *J. Hydraul. Eng.*, 2020, **146**(10), 04020069.
16. Ataie-Ashtiani, B. and Aslani-Kordkandi, A., Flow field around single and tandem piers. *Flow, Turbul. Combust.*, 2013, **90**(3), 471–490.

17. Melville, B. W. and Sutherland, A. J., Design method for local scour at bridge piers. *J. Hydraul. Eng*., 1988, **114**(10), 1210–1226.
18. Tang, H. W., Wang, H., Liang, D. F., Lv, S. Q. and Yan, L., Incipient motion of sediment in the presence of emergent rigid vegetation. *J. Hydro-environ. Res.*, 2013, **3**, 202–208.
19. Yalin, M. S. and Karahan, E., Inception of sediment transport. *J. Hydraul. Div*., 1979, **105**(11), 1433–1443.
20. Sarkar, K., Chakraborty, C. and Mazumder, B. S., Space–time dynamics of bed forms due to turbulence around submerged bridge piers. *Stoch. Environ. Res. Risk Assess.*, 2015, **29**(3), 995–1017.
21. Sarkar, K., Chakraborty, C. and Mazumder, B. S., Variation of bed elevations due to turbulence around submerged cylinders in sand beds. *Environ. Fluid Mech*., 2016, **16**(3), 659–693.
22. Chavan, R., Huai, W. and Kumar, B., Alluvial channel hydrodynamics around tandem piers with downward seepage. *Front. Struct. Civ. Eng.*, 2020, **14**, 1445–1461.
23. Hoffmans, G. J. C. M. and Verheij, H. J., *Scour Manual*, Balkema, Rotterdam, The Netherlands, 1997, pp. 1–304.

ACKNOWLEDGEMENTS. We thank the Centre of Excellence on ‘Water Resources and Flood Management’ at the Sardar Vallabhbhai National Institute of Technology, Surat, India funded by TEQIP-II, Ministry of Education, Government of India (GoI), for support. The experimental facility used in this study developed through the Department of Science and Technology, Government of India funded research project on ‘Erosion of non-uniform unimodal and bimodal sediments’, which we duly acknowledge.

Received 11 May 2022; re-revised accepted 22 June 2023

doi: 10.18520/cs/v125/i11/1227-1234